Journal of Power Sources 195 (2010) 977–983

Contents lists available at ScienceDirect

Journal of Power Sources

journal homepage: www.elsevier.com/locate/jpowsour

A potential interconnect material for solid oxide fuel cells: $Nd_{0.75}Ca_{0.25}Cr_{0.98}O_{3-\delta}$

Yu Shen [a], Monan Liu [a], Tianmin He [a,*], San Ping Jiang [b]

[a] National Key Laboratory of Superhard Materials and College of Physics, Jilin University, 2519 Jiefang Road, Changchun 130012, PR China
[b] School of Mechanical and Aerospace Engineering, Nanyang Technological University, 50 Nanyang Avenue, 639798, Singapore

ARTICLE INFO

Article history:
Received 21 July 2009
Received in revised form 28 August 2009
Accepted 28 August 2009
Available online 4 September 2009

Keywords:
Solid oxide fuel cell
Interconnect
Cr-deficiency
Sintering
Electrical property
Thermal expansion

ABSTRACT

Chromium-deficient $Nd_{0.75}Ca_{0.25}Cr_{1-x}O_{3-\delta}$ ($0.02 \le x \le 0.06$) oxides are synthesized and assessed as a novel ceramic interconnect for solid oxide fuel cells (SOFCs). At room temperature, all the samples present single perovskite phase after sintering at 1600 °C for 10 h in air. Cr-deficiency significantly improves the electrical conductivity of $Nd_{0.75}Ca_{0.25}Cr_{1-x}O_{3-\delta}$ oxides. No structural transformation occurs in the $Nd_{0.75}Ca_{0.25}Cr_{1-x}O_{3-\delta}$ oxides in the temperature range studied. Among all the samples, the $Nd_{0.75}Ca_{0.25}Cr_{0.98}O_{3-\delta}$ sample with a relative density of 96.3% exhibits the best electrical conductivity of 39.0 and 1.6 S cm^{-1} at 850 °C in air and hydrogen, respectively. The thermal expansion coefficient of $Nd_{0.75}Ca_{0.25}Cr_{0.98}O_{3-\delta}$ sample is 9.29×10^{-6} K^{-1} in the temperature range from 30 to 1000 °C in air, which is close to that of 8 mol% yttria stabilized zirconia electrolyte (10.3×10^{-6} K^{-1}) and other cell components. The results indicate that $Nd_{0.75}Ca_{0.25}Cr_{0.98}O_{3-\delta}$ is a potential interconnect material for SOFCs.

1. Introduction

Solid oxide fuel cells (SOFCs) are the most efficient devices yet invented for conversion of chemical fuels directly into electrical power, have attracted global attention over the past two decades with high energy conversion efficiency and an extremely low level of pollutant emissions [1]. However, the open-circuit voltage of an individual SOFC is low (around 1 V), thus interconnect material is used to connect individual cells in series and in parallel to realize high output voltages, currents and powers. As the operating temperature of SOFC is high (typically 800–1000 °C), the interconnect material must possess high electronic conductivity and negligible ionic conductivity, good chemical stability in both oxidizing and reducing atmospheres, and a thermal expansion coefficient (TEC) matched with other cell components in the operating temperature, as well as high density to prevent cross leakage of fuel and oxidant gases [2–4].

Because of the rigorous requirements for interconnect of SOFCs, only a few such oxides could be used as interconnect materials. Alkaline-earth (AE)-doped $MCrO_3$ (M = La, Y and Pr) are mostly used ceramic interconnect materials for high temperature SOFCs, as they show excellent electrical conductivity, high densification and high chemical stability in both oxidizing and reducing environments [5–7]. However, a structural transformation from orthorhombic phase to rhombohedral phase exists in $LaCrO_3$ and the AE-doped lanthanum chromites with the low AE contents. The increase of AE contents will result in a higher TEC for AE-doped lanthanum chromites, which causes thermal stress in SOFC and thus decreases its long-term stability performance [8–10]. The praseodymium in $PrCrO_3$-based oxides exists in the two valence states, Pr^{3+} and Pr^{4+} [11], which decreases the chemical stability. Recently, $La_{0.7}Ca_{0.3}CrO_3$ and doped CeO_2 composite was also considered as an interconnect material in SOFCs, in the case of the negligible oxygen ion conduction [12–14].

Little attention has been given to the sintering and electrical conductivity of AE-doped $NdCrO_3$ materials. Hirota et al. [15] fabricated Ca-doped $NdCrO_3$ interconnect materials using citric acid as a gelling agent, and showed high electrical conductivity and good sinterability. However, the procedure based on citric acid as a gelling agent is complex and may have limitation to the mass production of the oxides. Therefore the authors have prepared $Nd_{1-x}Ca_xCrO_3$ ($0 \le x \le 0.25$) oxides using simple two-step calcination solid-state reaction method, and the results indicated that the composition $Nd_{0.75}Ca_{0.25}CrO_3$ is a promising candidate as an interconnect material for application in SOFCs [16]. In the same way, we synthesized the $Nd_{1-x}Sr_xCrO_3$ oxides to investigate the feasibility of this material as interconnect for SOFC [17]. It is well known that $LaCrO_3$-based materials are poorly sinterable in air because of the chromium vaporization of the $LaCrO_3$-based oxides. Specifically, the poor sinterability of lanthanum chromite is attributed to a volatile species, such as CrO_3, forming and then being reduced to form solid Cr_2O_3 on the particle surface, which then inhibits sintering of the particles [18]. The sintering can be improved by using a chromium-deficient composition along with either

* Corresponding author. Fax: +86 431 88498000.
E-mail address: hly@mail.jlu.edu.cn (T. He).

0378-7753/$ – see front matter © 2009 Elsevier B.V. All rights reserved.
doi:10.1016/j.jpowsour.2009.08.090

calcium [19] or strontium [20] doping. Sakai et al. [21] reported that a slight amount of Ca substituting Cr site (y = 0–0.03) can drastically improve densification of the materials $(La_{1-x}Ca_x)(Cr_{1-y}Ca_y)O_3$ sintered at 1600 °C in air. This effect was explained due to the influence of Cr-deficiency (y value), which means that Cr-deficiency has a great influence on the properties of the materials. Wang et al. [22,23] also confirmed that a small amount of Cr-deficiency significantly improved the sintering ability in air and the electrical conductivity of $La_{0.7}Ca_{0.3}Cr_{1-x}O_{3-\delta}$. The Cr-deficiency may affect not only the crystal structure, but also the electrical conductivity and the thermal expansion, and thus must be understood and controlled in the development of ceramic interconnect materials for SOFCs.

In this paper, we synthesized Cr-deficient $Nd_{0.75}Ca_{0.25}Cr_{1-x}O_{3-\delta}$ ($0.02 \le x \le 0.06$) oxides using a two-step calcinations solid-state reaction method. The influence of Cr-deficiency on the crystal structure, sintering, electrical conductivity and thermal expansion behavior of the samples were investigated. The results show that composition $Nd_{0.75}Ca_{0.25}Cr_{0.98}O_{3-\delta}$ reveals superior properties and is a potential candidate as interconnect for application in SOFCs.

2. Experimental

2.1. Sample preparation

$Nd_{0.75}Ca_{0.25}Cr_{1-x}O_{3-\delta}$ ($0.02 \le x \le 0.06$) oxides were synthesized with a two-step calcinations solid-state reaction method using $CaCO_3$ (99%), Cr_2O_3 (99%) and Nd_2O_3 (99%) as starting materials as described previously [16]. Briefly, Cr_2O_3 and Nd_2O_3 were preheated at 900 °C for 2 h to remove the possible absorption of water and CO_2. The starting powders were weighed according to the composition $Nd_{0.75}Ca_{0.25}Cr_{1-x}O_{3-\delta}$, x = 0.02, 0.04 and 0.06, respectively. The mixtures were ground thoroughly in an agate mortar, followed by pelletization and calcination at 1000 and 1200 °C for 10 h, respectively. The reground powders were uniaxially pressed into pellets (⌀ 13 mm × 1 mm) at 220 MPa for the conductivity measurement and cylinders (⌀ 5 mm × 6 mm) for the thermal expansion measurement. These samples were finally sintered at 1600 °C for 10 h.

2.2. Characterization of samples

The powder diffraction data of the sintered samples were obtained from X-ray diffraction (XRD) measurements using a Rigaku-D-Max γA 12 kW X-ray diffractometer with CuKα radiation (λ = 0.15418 nm). The scan covered a 2θ range of 20–80° with a step size of 0.02°. To investigate the cyclic stability of $Nd_{0.75}Ca_{0.25}Cr_{0.98}O_{3-\delta}$ as interconnect, the sample was examined with X-ray diffraction after annealing at 900 °C for 20 h in 5%H_2/Ar. Further XRD studies were also carried out to investigate the chemical compatibility of $Nd_{0.75}Ca_{0.25}Cr_{0.98}O_{3-\delta}$ with anode NiO/YSZ (8 mol% yttria stabilized zirconia) and cathode $La_{0.8}Sr_{0.2}MnO_3$. The powder mixtures of $Nd_{0.75}Ca_{0.25}Cr_{0.98}O_{3-\delta}$ with NiO/YSZ (55:45) and $La_{0.8}Sr_{0.2}MnO_3$, in a weight ratio of 1:1, were ground in an agate mortar and fired at 1200 °C for 10 h. The bulk densities of the sintered samples were measured according to the Archimedes principle with deionized water as the immersion medium. The dc electrical conductivity of the samples was determined by a standard four-probe technique in the temperature range of 300–850 °C in air and in hydrogen, respectively. Microstructures of the samples sintered at 1600 °C for 10 h were inspected using a scanning electron microscopy (SEM) (JEOL JSM-6480LV). The thermal expansion behavior of the sintered samples was measured in air using a rod pushing dilatometer (Netzsch DIL 402C) in the temperature range

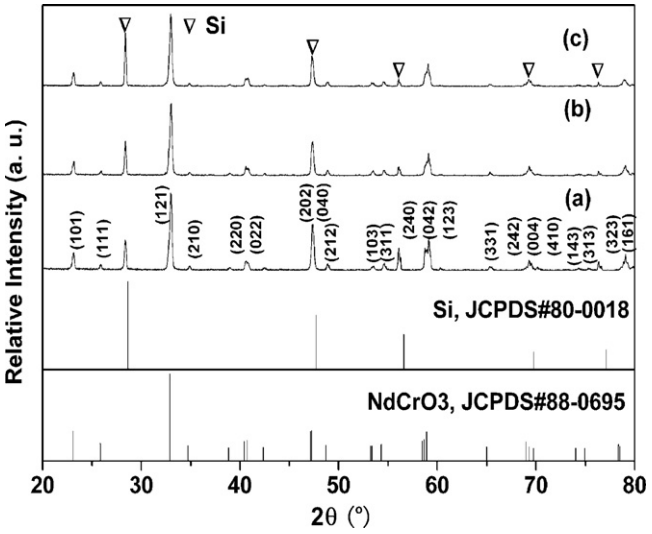

Fig. 1. XRD patterns of $Nd_{0.75}Ca_{0.25}Cr_{1-x}O_{3-\delta}$ ($0.02 \le x \le 0.06$) oxides after sintering at 1600 °C for 10 h. (a) x = 0.02; (b) x = 0.04; and (c) x = 0.06.

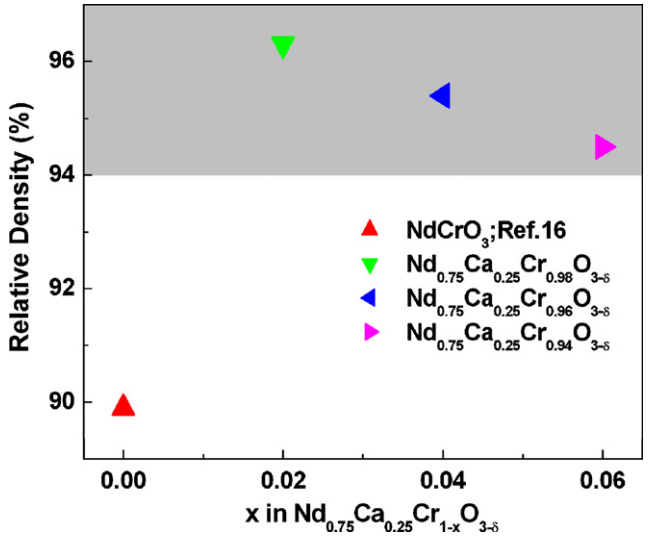

Fig. 2. Relative density of $NdCrO_3$ and $Nd_{0.75}Ca_{0.25}Cr_{1-x}O_{3-\delta}$ oxides after sintering at 1600 °C for 10 h. The relative density data of $NdCrO_3$ were taken from Ref. [16].

Table 1
Lattice parameters and cell volume of $Nd_{0.75}Ca_{0.25}Cr_{1-x}O_{3-\delta}$ oxides.

Samples	Lattice parameters			Cell volume (nm^3)
	a (nm)	b (nm)	c (nm)	
$NdCrO_3$ (JCPDS#88-0695)	0.5479	0.7691	0.5422	0.22854
$Nd_{0.75}Ca_{0.25}Cr_{0.98}O_{3-\delta}$	0.5414 (2)	0.7599 (9)	0.5365 (9)	0.22079 (9)
$Nd_{0.75}Ca_{0.25}Cr_{0.96}O_{3-\delta}$	0.5417 (6)	0.7599 (0)	0.5364 (9)	0.22086 (9)
$Nd_{0.75}Ca_{0.25}Cr_{0.94}O_{3-\delta}$	0.5417 (3)	0.7602 (5)	0.5367 (6)	0.22106 (9)

from 30 to 1000 °C, at a heating rate of 5 °C min^{-1} and a flow rate of 60 ml min^{-1} of air.

3. Results and discussion

3.1. X-ray powder diffraction

Fig. 1 shows the XRD patterns of $Nd_{0.75}Ca_{0.25}Cr_{1-x}O_{3-\delta}$ ($0.02 \le x \le 0.06$) samples after sintering at 1600 °C for 10 h. In order to calculate the lattice parameters of $Nd_{0.75}Ca_{0.25}Cr_{1-x}O_{3-\delta}$ accurately, the high-purity Si was used as an internal standard. It can be seen that the single-phase oxides have been obtained. All the reflections of these materials can be indexed as an orthorhombic perovskite structure at room temperature.

The unit cell lattice parameters of the samples were determined with a least-square refinement from the XRD patterns and the results are shown in Table 1. It can be seen that the lattice parameters decrease as a chromium-deficient content along with calcium doping in $NdCrO_3$ compared with pure $NdCrO_3$ (JCPDS#88-0695). This results from many competing factors such as the ionic radius of the acceptor dopant (Ca^{2+}), the mixed valence state of the chromium ion, and the oxygen deficiency. The substitution of the larger Ca^{2+} (0.134 nm) for Nd^{3+} (0.127 nm) at lattice positions should cause an incremental increase in the unit cell volume. On the other hand, when trivalent Nd^{3+} ions are partially replaced by divalent Ca^{2+} ions in $NdCrO_3$, some Cr^{3+} will change into Cr^{4+} or Cr^{6+} due to the charge compensation [24]. The ionic radii of Ca^{2+}, Nd^{3+}, Cr^{3+}, Cr^{4+} and Cr^{6+} are 0.134, 0.127, 0.0615, 0.055 and 0.044 nm (dodecahedral coordination for $Ca^{2+}$and Nd^{3+}; sixfold coordination for Cr^{3+}, Cr^{4+} and Cr^{6+}), respectively [25]. By comparing the sizes of the relevant ions, it is clear that the amount of the relative increment in the unit cell volume due to the substitution of larger Ca^{2+} is less than that of the relative decrement caused by the formation of chromium ions, which lead to the lattice contraction. In addition, we can see that the unit cell volume of the samples increase with the increasing chromium-deficiency content. This is

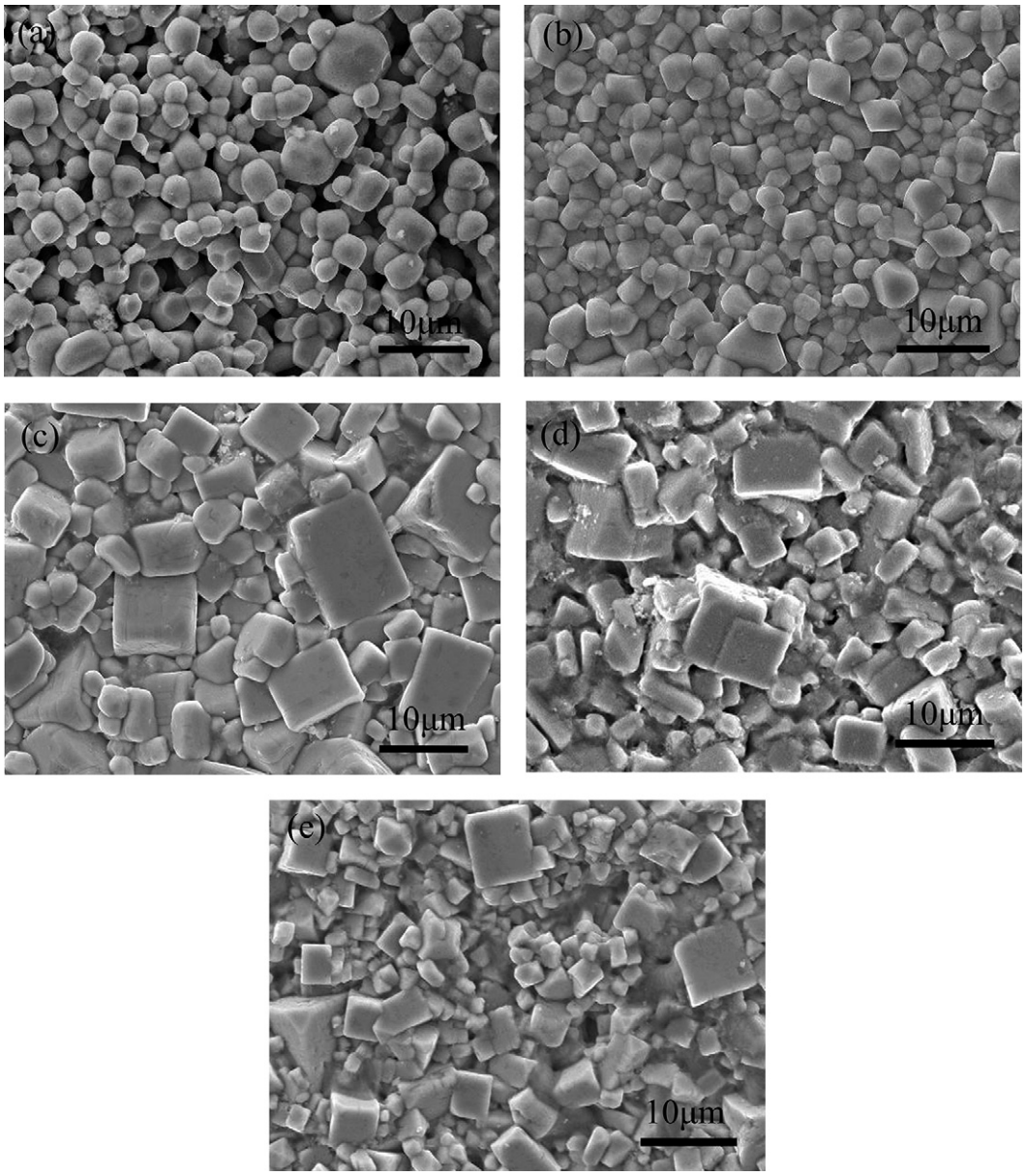

Fig. 3. SEM micrographs of $NdCrO_3$, $Nd_{0.75}Ca_{0.25}CrO_3$ and $Nd_{0.75}Ca_{0.25}Cr_{1-x}O_{3-\delta}$ oxides after sintering at 1600 °C for 10 h in air. (a) $NdCrO_3$; (b) $Nd_{0.75}Ca_{0.25}CrO_3$; (c) $Nd_{0.75}Ca_{0.25}Cr_{0.98}O_{3-\delta}$; (d) $Nd_{0.75}Ca_{0.25}Cr_{0.96}O_{3-\delta}$; and (e) $Nd_{0.75}Ca_{0.25}Cr_{0.94}O_{3-\delta}$. The SEM data of $NdCrO_3$ and $Nd_{0.75}Ca_{0.25}CrO_3$ were taken from Ref. [16].

mainly because the Cr-vacancy increases with the increase of the chromium-deficient content, thus resulting in the increase of the unit cell volume.

3.2. Sintering and microstructure

Because the interconnect material is to separate the fuel gas from the oxidant, a high density of interconnects should be maintained throughout their service time. For application as interconnect in SOFCs, the relative density of ceramic interconnects in the SOFCs should be ≥94% [26]. Fig. 2 shows the relative density of $NdCrO_3$ and $Nd_{0.75}Ca_{0.25}Cr_{1-x}O_{3-\delta}$ oxides after sintering at 1600 °C for 10 h. The relative density data of $NdCrO_3$ were taken from Ref. [16]. The sintering ability of the samples was greatly improved by a chromium-deficient composition along with calcium doping in $NdCrO_3$. Among these materials, $Nd_{0.75}Ca_{0.25}Cr_{0.98}O_{3-\delta}$ sample presents the highest relative density of 96.3%, which is sufficient for interconnect material for application in SOFCs.

Fig. 3 shows the SEM micrographs of $NdCrO_3$, $Nd_{0.75}Ca_{0.25}CrO_3$ [16] and $Nd_{0.75}Ca_{0.25}Cr_{1-x}O_{3-\delta}$ oxides after sintering at 1600 °C for 10 h in air. It can be seen that the sinterability of the samples was greatly improved by Ca dopant and Cr-deficiency in B site. Pure $NdCrO_3$ consists of symmetrical and equiaxial grains, however, the porosity in the sample is distinctly visible. With the calcium doping in $NdCrO_3$ oxides, the geometric shape of the $Nd_{0.75}Ca_{0.25}CrO_3$ grain changes, and the porosity in the samples decreases significantly. Interestingly, a well-defined, brick-shaped grain with a size of 1–12 μm is observed in the $Nd_{0.75}Ca_{0.25}Cr_{1-x}O_{3-\delta}$ oxides sintered at 1600 °C for 10 h. Comparing to the $Nd_{0.75}Ca_{0.25}CrO_3$ sample, however, a distinctly abnormal grain growth and decreased sintering density is observed in the $Nd_{0.75}Ca_{0.25}Cr_{1-x}O_{3-\delta}$ samples sintered at 1600 °C for 10 h. This might be indicative of an over-sintering phenomenon (abnormal grain growth due to over-sintering that results in a decrease in density [27]) that occurred in sintered samples [28]. On the other hand, the appearance of a little porosity is most likely due to the chromium volatilization at high temperature, in particular, the loss of Cr^{6+} ions, as CrO_3 molecules [29]. This fact suggests that the optimal sintering temperature for

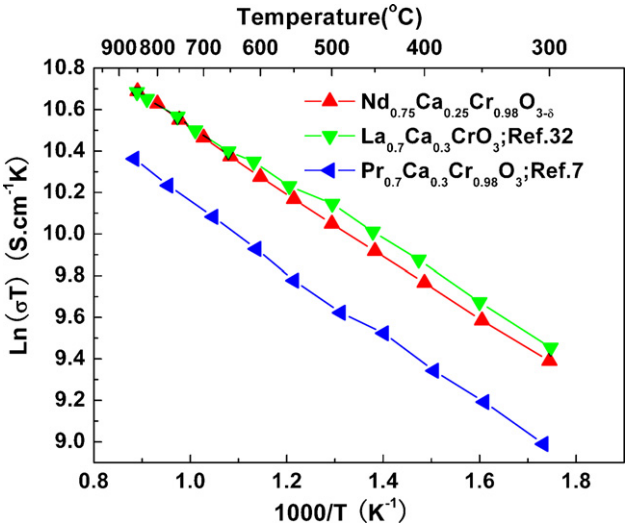

Fig. 5. Temperature dependence of the electrical conductivity of $Nd_{0.75}Ca_{0.25}Cr_{0.98}O_{3-\delta}$, $La_{0.7}Ca_{0.3}CrO_3$ and $Pr_{0.7}Ca_{0.3}Cr_{0.98}O_3$ measured in air. The conductivity data of $La_{0.7}Ca_{0.3}CrO_3$ and $Pr_{0.7}Ca_{0.3}Cr_{0.98}O_3$ were taken from Refs. [32] and [7], respectively.

$Nd_{0.75}Ca_{0.25}Cr_{1-x}O_{3-\delta}$ oxides should be reduced due to the Cr-deficiency facilitating the densification sintering [21–23].

3.3. Electrical conductivity

Fig. 4 shows the temperature dependence of the electrical conductivity for $NdCrO_3$, $Nd_{0.75}Ca_{0.25}CrO_3$ and $Nd_{0.75}Ca_{0.25}Cr_{1-x}O_{3-\delta}$ oxides in air. The conductivity data of $NdCrO_3$ and $Nd_{0.75}Ca_{0.25}CrO_3$ were taken from Ref. [16]. All the samples exhibited linear conductivity behavior in the temperature range from 300 to 850 °C. The linear relationship between $\ln(\sigma T)$ and $1/T$ (where σ is the electrical conductivity and T is the absolute temperature) indicates that the electrical conductivity behavior obeys the small-polaron conductivity mechanism [30]. And the nature of the electrical conductivity

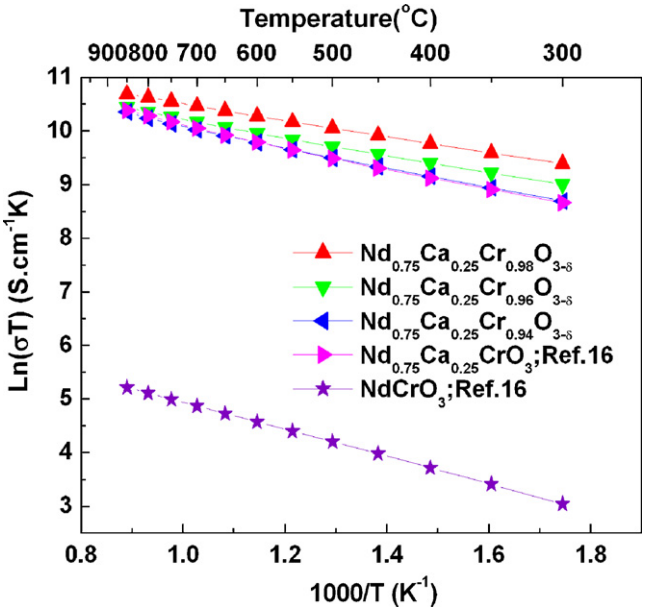

Fig. 4. Temperature dependence of the electrical conductivity of $NdCrO_3$, $Nd_{0.75}Ca_{0.25}CrO_3$ and $Nd_{0.75}Ca_{0.25}Cr_{1-x}O_{3-\delta}$ oxides, measured in air. The conductivity data of $NdCrO_3$ and $Nd_{0.75}Ca_{0.25}CrO_3$ were taken from Ref. [16].

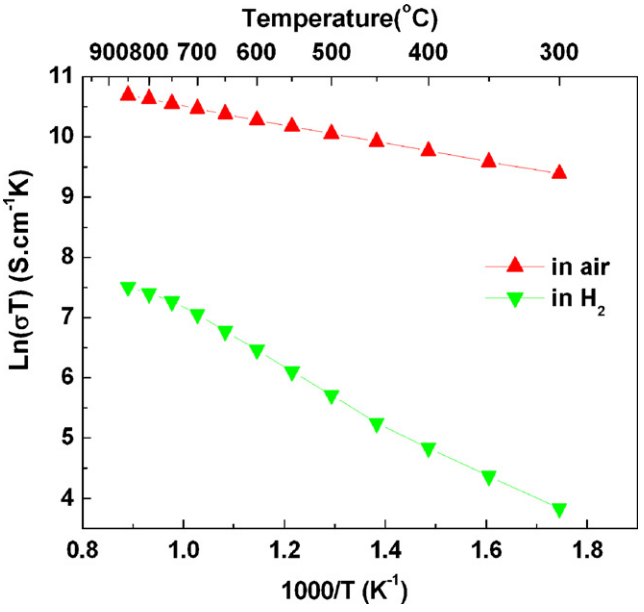

Fig. 6. Temperature dependence of the electrical conductivity of $Nd_{0.75}Ca_{0.25}Cr_{0.98}O_{3-\delta}$ oxide measured in air and H_2.

Table 2
Density, electrical conductivity and thermal expansion coefficient (TEC) of $Nd_{0.75}Ca_{0.25}Cr_{1-x}O_{3-\delta}$ oxides.

Samples	Theoretical density ($g\,cm^{-3}$)	Bulk density ($g\,cm^{-3}$)	Relative density (%)	Electrical conductivity at 850 °C ($S\,cm^{-1}$)	Activation energy (eV)	TEC (30–1000 °C) ($\times10^{-6}\,K^{-1}$)
$Nd_{0.75}Ca_{0.25}Cr_{0.98}O_{3-\delta}$	6.566	6.323	96.3	39.0	0.13	9.29
$Nd_{0.75}Ca_{0.25}Cr_{0.96}O_{3-\delta}$	6.564	6.265	95.4	30.5	0.14	9.35
$Nd_{0.75}Ca_{0.25}Cr_{0.94}O_{3-\delta}$	6.558	6.196	94.5	28.7	0.17	9.56

of Ca-doped $NdCrO_3$ can be expressed as (in the Kröger–Vink notation) [4]:

$$[Ca'_{Nd}] = [Cr_{Cr}^{\bullet}] \quad (1)$$

where [ ] represents concentration, $Cr_{Cr}^{\bullet}$ is Cr^{4+} in Cr site.

The electrical conductivities of $Nd_{0.75}Ca_{0.25}CrO_3$ and $Nd_{0.75}Ca_{0.25}Cr_{1-x}O_{3-\delta}$ oxides are greatly improved compared with pure $NdCrO_3$. This can be understood as a result of the substitution of the Ca^{2+} for Nd^{3+} increases the concentration of $Cr_{Cr}^{\bullet}$ *via* electronic compensation mechanism. Similar to the Ca dopant in $NdCrO_3$, the Cr-deficiency in $Nd_{0.75}Ca_{0.25}Cr_{1-x}O_{3-\delta}$ will also increase the concentration of $Cr_{Cr}^{\bullet}$, which results in the higher electrical conductivity of $Nd_{0.75}Ca_{0.25}Cr_{1-x}O_{3-\delta}$ oxides than that of $Nd_{0.75}Ca_{0.25}CrO_3$. From Fig. 4 it can also be seen that the electrical conductivity of $Nd_{0.75}Ca_{0.25}Cr_{1-x}O_{3-\delta}$ decreases with the increase of the Cr-deficiency content. As the increase of Cr-deficiency content, the concentration of Cr-vacancy will increase. The negatively charged Cr-vacancy might has the tendency to attract the positively charged $Cr_{Cr}^{\bullet}$ to keep micro electrical neutrality, so that the small-polaron hopping of $Cr_{Cr}^{\bullet}$ is confined, leading to decrease of the electrical conductivity ability in the materials when the Cr-deficiency content increases [22].

The selected electrical conductivity data of $Nd_{0.75}Ca_{0.25}Cr_{1-x}O_{3-\delta}$ oxides at 850 °C in air are shown in Table 2. Among these materials, $Nd_{0.75}Ca_{0.25}Cr_{0.98}O_{3-\delta}$ shows the superior electrical conductivity with 39.0 S cm^{-1} at 850 °C, which is higher than that of $Nd_{0.75}Ca_{0.25}CrO_3$ (28.8 S cm^{-1} at 850 °C) [16]. The conductivity values of the $Nd_{0.75}Ca_{0.25}Cr_{1-x}O_{3-\delta}$ oxides are also significantly higher that of $Y_{0.7}Ca_{0.3}Cr_{0.9}Zn_{0.1}O_{3-\delta}$ (20.9 S cm^{-1} at 850 °C in air), a novel interconnect material recently reported by Wang et al. [31]. In addition, we can note that the electrical conductivity of $Nd_{0.75}Ca_{0.25}Cr_{1-x}O_{3-\delta}$ oxides decreases as the Cr-deficiency content is increased. We can see from Fig. 2 and Table 2, the sintered density of $Nd_{0.75}Ca_{0.25}Cr_{1-x}O_{3-\delta}$ oxides decreases with the increasing of the Cr-deficiency content, thus reducing the electrical conductivity of $Nd_{0.75}Ca_{0.25}Cr_{1-x}O_{3-\delta}$ oxides.

Fig. 5 compares the electrical conductivity for $Nd_{0.75}Ca_{0.25}Cr_{0.98}O_{3-\delta}$, $La_{0.7}Ca_{0.3}CrO_3$ and $Pr_{0.70}Ca_{0.30}Cr_{0.98}O_3$ oxides measured in air. The conductivity data of $La_{0.7}Ca_{0.3}CrO_3$ and $Pr_{0.70}Ca_{0.30}Cr_{0.98}O_3$ were taken from Refs. [32] and [7], respectively. The electrical conductivity of $Nd_{0.75}Ca_{0.25}Cr_{0.98}O_{3-\delta}$ is higher than that of $Pr_{0.70}Ca_{0.30}Cr_{0.98}O_3$ in Ref. [7] and close to that of $La_{0.7}Ca_{0.3}CrO_3$ in Ref. [32]. It is well known that the current density is limited by the minimal conductivity in the fuel cell stacks [4]. The conductivity of interconnect is the lowest among the adjacent anode and cathode components, so the high conductivity of $Nd_{0.75}Ca_{0.25}Cr_{0.98}O_{3-\delta}$ can decrease the ohmic loss in the SOFCs. This means that $Nd_{0.75}Ca_{0.25}Cr_{0.98}O_{3-\delta}$ is a very promising candidate as the interconnect material for application in SOFCs.

Fig. 6 shows the electrical conductivity of $Nd_{0.75}Ca_{0.25}Cr_{0.98}O_{3-\delta}$ measured at different temperatures in hydrogen. The electrical conductivity of $Nd_{0.75}Ca_{0.25}Cr_{0.98}O_{3-\delta}$ shows a noticeable decrease in H_2 as compared with that in air. It has been reported that $LaMO_3$ (M = transition metals)-based perovskite structure has a non-stoichiometry at the oxygen site at low oxygen partial pressure of 10^{-8}–10^{-18} atm [33,34]. Under a reducing atmosphere, a charge compensation of Cr^{4+} to Cr^{3+} ions occurs by the formation of oxygen vacancies, which leads to the decrease of the electrical conductivity as the concentration of small polarons decreases. The electrical conductivity of $Nd_{0.75}Ca_{0.25}Cr_{0.98}O_{3-\delta}$ is 1.6 S cm^{-1} at 850 °C in hydrogen, above the well-accepted minimum electrical conductivity of 1 S cm^{-1} for the interconnect application in SOFCs [35]. Thus, the electrical conductivity of $Nd_{0.75}Ca_{0.25}Cr_{0.98}O_{3-\delta}$ in reducing atmosphere is also sufficient as an interconnect material for application in SOFCs.

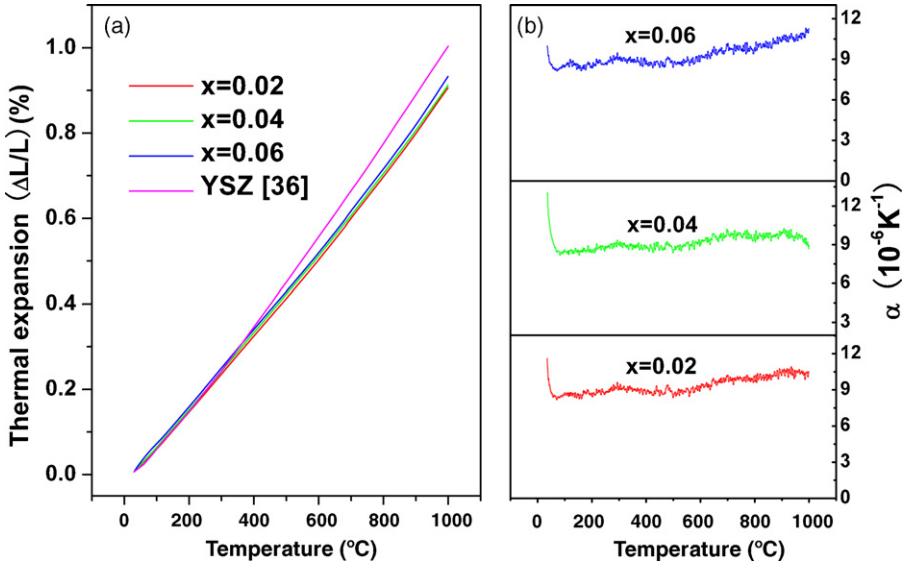

Fig. 7. (a) Thermal expansion curves of $Nd_{0.75}Ca_{0.25}Cr_{1-x}O_{3-\delta}$ oxides and YSZ electrolyte and (b) thermal expansion coefficient curves of $Nd_{0.75}Ca_{0.25}Cr_{1-x}O_{3-\delta}$ oxides. The thermal expansion data of YSZ were taken from Ref. [36].

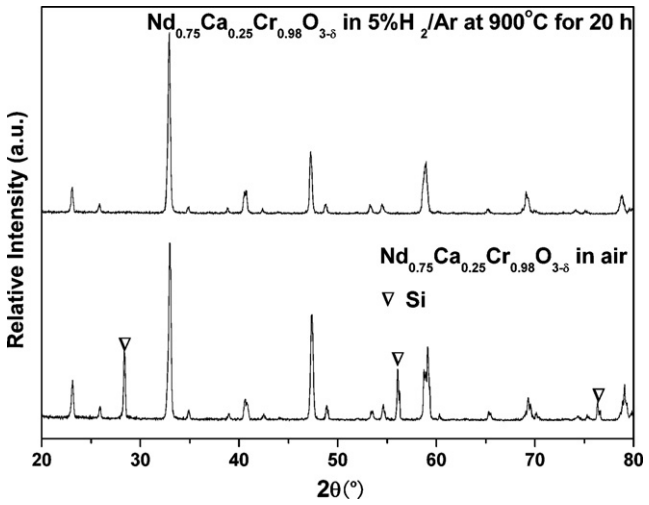

Fig. 8. XRD patterns of $Nd_{0.75}Ca_{0.25}Cr_{0.98}O_{3-\delta}$ sample (a) in air and (b) after annealing at 900 °C for 20 h in 5%H_2/Ar.

3.4. Thermal expansion

Since SOFCs operate at high temperatures and should endure the thermal cycle from room temperature to operating temperature, interconnects must be thermally compatible with the other cell components. Therefore, the TEC of SOFC interconnects must be close to those of the other cell components to minimize the thermal stresses. Fig. 7(a) shows the thermal expansion curves of $Nd_{0.75}Ca_{0.25}Cr_{1-x}O_{3-\delta}$ oxides and YSZ electrolyte in the temperature range of 30–1000 °C in air. To identify the volume change of the $Nd_{0.75}Ca_{0.25}Cr_{1-x}O_{3-\delta}$ oxides, the thermal expansion coefficient curves are shown in Fig. 7(b). The data of thermal expansion of YSZ were taken from Ref. [36]. It can be seen from Fig. 7 that there is no inflection in the thermal expansion curves. Also there is no remarkably abrupt change occurring in the thermal expansion coefficient curves. This indicates that no structural transition appeared in the $Nd_{0.75}Ca_{0.25}Cr_{1-x}O_{3-\delta}$ oxides studied here. The TECs of $Nd_{0.75}Ca_{0.25}Cr_{1-x}O_{3-\delta}$ oxides increase with the increase of the Cr-deficiency content. As mentioned above, the increase of Cr-deficiency content will increase the concentration of Cr-vacancy. Therefore the increase of Cr-vacancy increases the TECs of the $Nd_{0.75}Ca_{0.25}Cr_{1-x}O_{3-\delta}$ samples which are the same as the effects of oxygen vacancy on the TECs [37]. The values of TEC for $Nd_{0.75}Ca_{0.25}Cr_{1-x}O_{3-\delta}$ oxides are shown in Table 2. The TEC values of $Nd_{0.75}Ca_{0.25}Cr_{1-x}O_{3-\delta}$ oxides are in the range of 9.29–9.56 $\times 10^{-6}$ K^{-1} and increase with the increase of Cr-deficiency content. This is in good agreement with the increase of the unit cell volume. The TEC of sample $Nd_{0.75}Ca_{0.25}Cr_{0.98}O_{3-\delta}$ is 9.29 $\times 10^{-6}$ K^{-1} in the temperature range from 30 to 1000 °C in air, which is close to that of the YSZ electrolyte (10.3 $\times 10^{-6}$ K^{-1}) [36]. The TEC is also fairly compatible with those of adjoining components, such as the most commonly used Ni-YSZ anode (10.8 $\times 10^{-6}$ K^{-1}) [22] and Sr-doped $LaMnO_3$ cathode (11.2–12.7 $\times 10^{-6}$ K^{-1}) [38] in SOFCs.

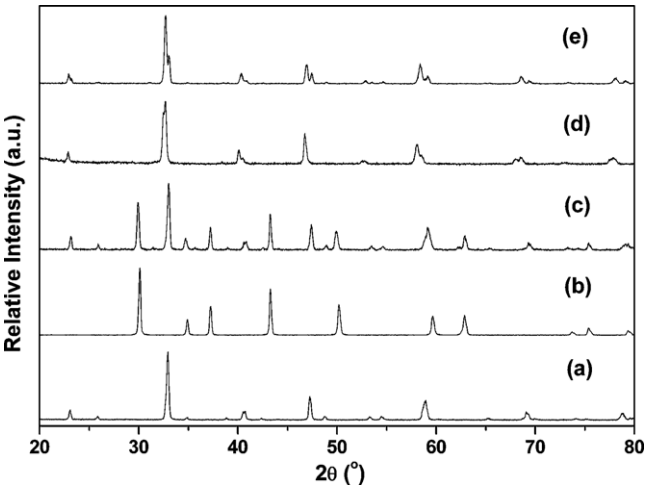

Fig. 9. XRD patterns of $Nd_{0.75}Ca_{0.25}Cr_{0.98}O_{3-\delta}$-NiO/YSZ and $Nd_{0.75}Ca_{0.25}Cr_{0.98}O_{3-\delta}$–$La_{0.8}Sr_{0.2}MnO_3$ mixtures after sintering at 1200 °C for 10 h in air. (a) $Nd_{0.75}Ca_{0.25}Cr_{0.98}O_{3-\delta}$ sintered at 1600 °C for 10 h; (b) NiO/YSZ sintered at 1100 °C for 6 h; (c) $Nd_{0.75}Ca_{0.25}Cr_{0.98}O_{3-\delta}$–NiO/YSZ mixtures sintered at 1200 °C for 10 h; (d) $La_{0.8}Sr_{0.2}MnO_3$ sintered at 1100 °C for 6 h; and (e) $Nd_{0.75}Ca_{0.25}Cr_{0.98}O_{3-\delta}$–$La_{0.8}Sr_{0.2}MnO_3$ mixtures sintered at 1200 °C for 10 h.

3.5. Cyclic stability and chemical compatibility

Fig. 8 shows the XRD patterns of $Nd_{0.75}Ca_{0.25}Cr_{0.98}O_{3-\delta}$ sample (a) in air and (b) after annealing at 900 °C for 20 h in 5%H_2/Ar. It can be seen from Fig. 8 that no second phase was observed after this treatment. This fact suggests that $Nd_{0.75}Ca_{0.25}Cr_{0.98}O_{3-\delta}$ oxide is chemically stable under reducing atmospheres at high temperatures. Fig. 9 shows the XRD patterns of $Nd_{0.75}Ca_{0.25}Cr_{0.98}O_{3-\delta}$-NiO/YSZ and $Nd_{0.75}Ca_{0.25}Cr_{0.98}O_{3-\delta}$–$La_{0.8}Sr_{0.2}MnO_3$ mixtures after sintering at 1200 °C for 10 h in air. No additional diffraction peaks were found in the XRD patterns, which indicated that $Nd_{0.75}Ca_{0.25}Cr_{0.98}O_{3-\delta}$ had a good chemical compatibility with the adjacent anode and cathode.

4. Conclusions

The dense perovskite oxides $Nd_{0.75}Ca_{0.25}Cr_{1-x}O_{3-\delta}$ (0.02 × 0.06) were synthesized using a two-step calcinations solid-state reaction method. The influence of Cr-deficiency on the crystal structures, sintering, electrical conductivities and thermal expansion behaviors of the samples were investigated. All the samples presented single perovskite phase after sintering at 1600 °C for 10 h in air. The volume of unit cell and the TEC of $Nd_{0.75}Ca_{0.25}Cr_{1-x}O_{3-\delta}$ oxides increase with the increase of the Cr-deficiency content. No structural transformation occurred in the $Nd_{0.75}Ca_{0.25}Cr_{1-x}O_{3-\delta}$ oxides in the temperature range studied. Cr-deficiency can significantly improve the electrical conductivity of $Nd_{0.75}Ca_{0.25}Cr_{1-x}O_{3-\delta}$ oxides. Among these materials, $Nd_{0.75}Ca_{0.25}Cr_{0.98}O_{3-\delta}$ sample with a relative density of 96.3% showed the best electrical conductivity of 39.0 and 1.6 S cm^{-1} at 850 °C in air and hydrogen, respectively. The TEC of $Nd_{0.75}Ca_{0.25}Cr_{0.98}O_{3-\delta}$ is 9.29 $\times 10^{-6}$ K^{-1} in the temperature range from 30 to 1000 °C in air, which is close to those of the YSZ electrolyte and the other cell components. The obtained data indicate that $Nd_{0.75}Ca_{0.25}Cr_{0.98}O_{3-\delta}$ is a potential interconnect material for application in SOFCs.

Acknowledgement

This work was supported by the National Foundation for Fostering Talents of Basic Science under contract No. J0730311.

References

[1] S.C. Singhal, K. Kendall, High Temperature Solid Oxide Fuel Cells: Fundamentals, Design and Applications, Elsevier Advanced Technology, Oxford, 2003.
[2] N.Q. Minh, T. Takahashi, Science and Technology of Ceramic Fuel Cells, Elsevier Science B.V., New York, 1995, pp. 165–198.
[3] N.Q. Minh, J. Am. Ceram. Soc. 76 (1993) 563–588.
[4] W.Z. Zhu, S.C. Deevi, Mater. Sci. Eng. A 348 (2003) 227–243.
[5] M. Mori, T. Yamamoto, H. Itoh, T. Watanabe, J. Mater. Sci. 32 (1997) 2423–2431.
[6] G.F. Carini II, H.U. Anderson, D.M. Sparlin, M.M. Nasrallah, Solid State Ionics 49 (1991) 233–243.

[7] Z. Liu, D. Dong, X. Huang, Z. Lu, Y. Sui, X. Wang, J. Miao, Z.X. Shen, W. Su, Electrochem. Solid State Lett. 8 (2005) A250–A252.
[8] F. Nakamura, Y. Matsunaga, N. Ohba, K. Arai, H. Matsubara, H. Takahashi, T. Hashimoto, Thermochim. Acta 435 (2005) 222–229.
[9] M.N. Iliev, A.P. Litvinchuk, V.G. Hadjiev, Y.-Q. Wang, J. Cmaidalka, R.-L. Meng, Y.-Y. Sun, N. Kolev, M.V. Abrashev, Phys. Rev. B 74 (2006), 214301-1-7.
[10] N. Sakai, H. Yokokawa, T. Horita, K. Yamaji, Int. J. Appl. Ceram. Technol. 1 (2004) 23–30.
[11] Z. Liu, Z. Zheng, X. Huang, Z. Lu, T. He, D. Dong, Y. Sui, J. Miao, W. Su, J. Alloys Compd. 363 (2004) 61–63.
[12] X. Zhou, J. Ma, F. Deng, G. Meng, X. Liu, Solid State Ionics 177 (2007) 3461–3466.
[13] X. Zhou, F. Deng, M. Zhu, G. Meng, X. Liu, J. Power Sources 164 (2007) 293–299.
[14] X. Zhou, P. Wang, L. Liu, K. Sun, Z. Gao, N. Zhang, J. Power Sources 191 (2009) 377–383.
[15] K. Hirota, Y. Kunifusa, M. Yoshinaka, O. Yamaguchi, Mater. Res. Bull. 37 (2002) 2335–2344.
[16] Y. Shen, M. Liu, T. He, S. Jiang, J. Am. Ceram. Soc. (2009), doi:10.1111/j.1551-2916.2009.03196.x.
[17] M. Liu, Y. Shen, Y. Ji, T. He, J. Alloys Compd. 461 (2008) 628–632.
[18] H. Yokokawa, N. Sakai, T. Kawada, M. Dokiya, J. Electrochem. Soc. 138 (1991) 1018–1027.
[19] H. Yokokawa, Solid-State Ionics Devices III—Electrochem. Soc. Proc. vol. PV 2002-26, The Electrochemical Society, Pennington, NJ, 2002, pp. 1–15.
[20] S. Simner, J. Hardy, J. Stevenson, T. Armstrong, J. Mater. Sci. Lett. 19 (2000) 863–865.
[21] N. Sakai, T. Kawada, H. Yokokawa, M. Dokiya, J. Mater. Sci. 25 (1990) 4531–4534.
[22] S. Wang, M. Liu, Y. Dong, K. Xie, X. Liu, G. Meng, Mater. Res. Bull. 43 (2008) 2607–2616.
[23] S. Wang, B. Lin, K. Xie, Y. Dong, X. Liu, G. Meng, J. Alloys Compd. 468 (2009) 499–504.
[24] G.J. Zhang, H. Xiong, J.Y. Zheng, Y.Q. Jia, Y. Xuan, N. Mizutani, Mater. Chem. Phys. 71 (2001) 84–89.
[25] R.D. Shannon, Acta. Crystallogr. A 32 (1976) 751–767.
[26] B.K. Flandermeyer, J.T. Dusek, P.E. Blackburm, D.W. Dees, C.C. MacPheeters, R.B. Poeppel, Abstract of National Fuel Cell Seminar, Tucson, Arizona, Courtesy Associates, Washington, DC, 1986, p. 68.
[27] W.D. Kingery, H.K. Bowen, D.R. Uhlmann, Introduction to Ceramics, 2nd ed., Wiley, New York, 1976, p. 461.
[28] T. He, Z. Lu, Y. Huang, P. Guan, J. Liu, W. Su, J. Alloys Compd. 337 (2002) 231–236.
[29] M. Mori, Y. Hiei, N.M. Sammes, Solid State Ionics 123 (1999) 103–111.
[30] D.P. Karim, A.T. Aldred, Phys. Rev. B 20 (1979) 2255–2263.
[31] S. Wang, B. Lin, Y. Dong, D. Fang, H. Ding, X. Liu, G. Meng, J. Power Sources 188 (2009) 483–488.
[32] A. Chakraborty, R.N. Basu, H.S. Maiti, Mater. Lett. 45 (2000) 162–166.
[33] J. Mizusaki, S. Yamauchi, K. Fueki, A. Ishikawa, Solid State Ionics 12 (1984) 119–124.
[34] J. Mizusaki, Y. Mima, S. Yamauchi, K. Fueki, H. Tagawa, J. Solid State Chem. 80 (1989) 102–111.
[35] N.Q. Minh, C.R. Horne, F.S. Liu, M. Moffatt, R.R. Staszak, T.L. Stillwagon, J.J. Van Ackeren, Proceedings of the 25th Intersociety Energy Conversion Engineering Conference, vol. 3, American Institute of Chemical Engineers, New York, 1990, pp. 230–234.
[36] L. Cong, T. He, Y. Ji, P. Guan, Y. Huang, W. Su, J. Alloys Compd. 348 (2003) 325–331.
[37] S. Onuma, K. Yashiro, S. Miyoshi, A. Kaimai, H. Matsumoto, Y. Nigara, T. Kawada, J. Mizusaki, K. Kawamura, N. Sakai, H. Yokokawa, Solid State Ionics 174 (2004) 287–293.
[38] S. Jiang, J. Mater. Sci. 43 (2008) 6799–6833.